Dyes and Pigments 158 (2018) 277–284

Contents lists available at ScienceDirect

Dyes and Pigments

journal homepage: www.elsevier.com/locate/dyepig

Fluorescence *turn-on* detection of fluoride using HPQ-silyl ether reactive probes and its *in vivo* application

Yi Zhou[a,*], Meng-Meng Liu[a], Jing-Yun Li[b,c], Min-An Ye[a], Cheng Yao[a,**]

[a] College of Chemistry and Molecular Engineering, Nanjing Tech University, Nanjing, 211816, PR China
[b] Department of Plastic&Cosmetic Surgery, Maternal and Child Health Medical Institute, Obstetrics and Gynecology Hospital Affiliated to Nanjing Medical University, Nanjing, 210004, PR China
[c] State Key Laboratory of Pharmaceutical Biotechnology, MOE Key Laboratory of Model Animals for Disease Study, Model Animal Research Center of Nanjing University, Nanjing, 210061, PR China

ARTICLE INFO

Keywords:
In vivo imaging
Silyl ether
Steric hindrance
Probe
Fluoride

ABSTRACT

Fluoride and its derivatives are implicated in a variety of pathological and physiological conditions and hence play an important role in our daily life. Thus a fluorescent probe that enables the detection and imaging of fluoride in living species is highly demanded. In this study, three *turn-on* fluorescent probes (HPQF1 ~ HPQF3) were designed for detecting fluoride with their sensibilities verified by different steric hindrances around silyl ethers. The three HPQ-based probes could quantitatively detect fluoride anion in acetonitrile as well as in water. The fluorescent response time was only a few seconds in acetonitrile, and two different fluorescent sensing channels in acetonitrile (blue) and water (green) were observed by naked eyes. This work also provides a useful method to fluorescently image the presence of fluoride anions in both living cells and specific zebrafish organelles.

1. Introduction

Fluoride has received considerable attention due to its great potential in biological and industrial applications [1]. At a moderate concentration, its derivatives can effectively prevent prophylactic tooth decay and treat osteoporosis [2]. However, excessive ingestion of fluoride was proved to cause dental or skeletal fluorosis, gastric and kidney disorders, urolithiasis in humans, as well as inhibit neurotransmitter biosynthesis in fetuses [3]. Furthermore, fluoride is everywhere in our daily life as it is added to tap water and toothpaste and can also be released upon hydrolysis of phosphorofluoridate nerve agents, both of which make it urgent to assess the possible toxicity [4]. Thus, rapid and specific probes for quantitative detection of fluoride in water and living systems are of increasing importance in chemosensor research.

Recently, great efforts have been directed to the development of fluorescent sensors or probes for detecting fluoride. Among the existing analytical methods, three main strategies have been utilized for optical detection of fluoride include: hydrogen bonding between fluoride and NH hydrogen (amide, pyrrole, indole, urea, tetrazole and thiourea) [5], boron-fluoride complexation [6], and fluoride mediated desilylation [7,9,10]. The ionic strength and hydration enthalpy of fluoride in water are increased significantly [8], which makes hydrogen bonding ineffective in *aqueous* media. Though Organoboron-derived chemosensors could monitor fluoride in drinking water and fluorinated chemical warfare agents (e.g. Sarin) [6b], they are unsuitable for biological applications due to their cytotoxicity and instability in cellular environments [7f]. Considering the great affinity of fluoride for silicon, Kim and Swager firstly exploited *aqueous* fluoride chemosensors by using fluoride-triggered Si-O cleavage [9], which can alleviate the problems faced by the first two strategies and thus has received growing interest. A probe that can work in *aqueous* conditions and permeate cell membranes has not been realized until Hong's group developed a silyl ether-coumarin probe for detecting fluoride with the aid of this strategy [10a,12,13]. Nevertheless, those probes still need to be modified from the following considerations: (1) Compared with excited state intramolecular proton transfer ESIPT-based probes [7b,11], silyl ether-coumarin based probes cannot minimize background fluorescence and thus their sensitivity is decreased; (2) The rapid single-wavelength fluorescence response and determination with a low detection limit are still rare in *aqueous* media; (3) The component of silyl ethers *via* steric hindrance factor that governs selectivity and sensitivity has never been discussed in designing fluoride probes; (4) Chemosensor-based methodology for monitoring the accumulated fluoride in living organisms has

* Corresponding author.
** Corresponding author.
E-mail addresses: zhouyinjtech@njtech.edu.cn, zhouyinjtech@126.com (Y. Zhou), yaocheng@njtech.edu.cn, yaochengnjut@126.com (C. Yao).

https://doi.org/10.1016/j.dyepig.2018.05.053
Received 28 April 2018; Received in revised form 23 May 2018; Accepted 24 May 2018
Available online 25 May 2018
0143-7208/

not been established, which makes it difficult to assess the fluoride level of individual organs. These issues should be addressed when designing fluoride probes for biological applications.

2. Experimental section

2.1. Reagents and apparatus

Unless otherwise stated, all reagents were purchased from commercial suppliers and used without further purification. Solvents were purified and dried using standard procedures. Electrospray ionization mass spectra (*ESI-MS*) were measured on a Micromass LCTTM system. Fluorescence was measured at room temperature on a Perkin-Elmer LS 50B fluorescence spectrophotometer. ^{1}H NMR and ^{13}C NMR were measured on a BrukerAV-500 or BrukerAV-300 spectrometer with chemical shifts in ppm (in $CDCl_3$ or DMSO-d_6; TMS as internal standard). Data were presented as follows: Chemical shift (in ppm on the scale TMS as internal standard), integration, multiplicity (s = singlet, d = doublet, t = triplet, q = quartet, and m = multiplet), coupling constant (J/Hz), and interpretation. pH measurements was made with a Sartorius basic pH meter PB-10. Φ_F was determined with rhodamine B as a standard (Φ_F = 0.69 in ethanol). TLC analysis was performed on silica gel plates. Column chromatography was conducted over silica gel (mesh 200–300), and both were obtained from the Qingdao Ocean Chemicals.

2.2. Synthesis and characterization of probes

2-(2′-hydroxy-phenyl)-4(3H)-quinazolinone (**HPQ**): 2-Aminobenzamide (544 mg, 4.0 mmol) was dissolved in anhydrous EtOH (25 mL) and followed by the addition of salicylic aldehyde (488 mg, 4.0 mmol). The reaction mixture was refluxed in the presence of 2 drops of piperidine for 90 min. The resulting solution was cooled to 0 °C, and DDQ (2,3-dichloro-5,6-dicyano-1, 4-benzoquinone, 908 mg, 4.0 mmol) was added in 3 portions over 30 min. The mixture was slowly brought to room temperature for another 1 h and a greenish precipitate was formed. The solid was collected by filtration and washed with a small amount of cooled ethanol, which was purified by recrystallisation using ethanol to afford the desired pale yellow compound (819 mg, yield: 86%). M.p. 299.6–301.3 °C. ^{1}H NMR (300 MHz, DMSO-d_6): δ = 8.21 (m, 2H, Ar-H), 7.82 (m, 2H, Ar-H), 7.54 (m, 2H, Ar-H), 6.98 (m, 2H, Ar-H). *ESI*-MS: *m/z* 239.1 $[M+H]^+$, 261.1 $[M+Na]^+$.

2-(2′-tert-butyldimethylsilyloxy-phenyl)-4(3H)-quinazolinone (HPQF 1): To a solution of 2-(2′-hydroxy-phenyl)-4(3H)-quinazolinone **HPQ** (476 mg, 2.0 mmol) in anhydrous CH_2Cl_2 (40 mL), DMAP (4-dimethylamiopryidine, 30 mg) and triethylamine (0.8 mL) were added. The resulting mixture was cooled to 0 °C, and TBDMSCl (t-butyldimethylsilyl chloride, 450 mg, 3.0 mmol, in 10 ml CH_2Cl_2) was added in 3 portions over 30 min. The suspended mixture was slowly dissolved at room temperature with another 1 h. Then it was poured into the saturated $NaHCO_3$ (40 mL) solution, and the resulting mixture was extracted three times with CH_2Cl_2 (40 mL). The combined organic layer was dried over anhydrous Na_2SO_4, and concentrated under vacuum. Compound **HPQF 1** was isolated using a silica gel chromatographic column eluted with petroleum ether/Dichloromethane/ethyl acetate (v/v/v, 50:47:3), resulting a light yellow solid (R_f = 0.45, 148 mg, yield: 21%). ^{1}H NMR (300 MHz, $CDCl_3$): δ = 10.73 (s, 1H, N-H), 8.38 (d, J = 7.9 Hz, 1H, Ar-H), 8.31 (d, J = 7.9 Hz, 1H, Ar-H), 7.79 (m, 2H, Ar-H), 7.49 (t, J = 7.8 Hz, 1H, Ar-H), 7.41 (t, J = 7.8 Hz, 1H, Ar-H), 7.17 (t, J = 7.5 Hz, 1H, Ar-H), 6.98 (d, J = 8.2 Hz, 1H, Ar-H), 1.05 (s, 9H, -SiC$(CH_3)_3$), 0.338 (s, 6H, -Si$(CH_3)_2$). ^{13}C NMR (125 MHz, $CDCl_3$): 161.37, 154.01, 151.11, 149.43, 134.42, 132.62, 131.43, 129.98, 127.84, 126.48, 122.60, 122.45, 121.22, 120.37, 25.75, 18.37, −4.10. Anal. HPLC: 99.1% purity. Anal. Calcd for $C_{20}H_{24}N_2O_2Si$: C, 68.02; H, 6.51; N, 8.04. Found: C, 68.15; H, 6.86; N, 7.95. *ESI*-MS: *m/z* 353.1 $[M+H]^+$, 375.1 $[M+Na]^+$.

2-(2′-triisopropylsilyloxy-phenyl)-4(3H)-quinazolinone (**HPQF 2**): To a solution of 2-(2′-hydroxy-phenyl)-4(3H)-quinazolinone **HPQ** (476 mg, 2.0 mmol) in anhydrous CH_2Cl_2 (40 mL), DMAP (4-dimethylamiopryidine, 30 mg) and triethylamine (0.8 mL) were added. The resulting mixture was cooled to 0 °C, and TIPSCl (Triisopropylsilyl chloride, 576 mg, 3.0 mmol, in 10 ml CH_2Cl_2) was added in 3 portions over 30 min. The suspended mixture was slowly dissolved at room temperature with another 1 h. Then it was poured into the saturated $NaHCO_3$ (40 mL) solution, and the resulting mixture was extracted three times with CH_2Cl_2 (40 mL). The combined organic layer was dried over anhydrous Na_2SO_4, and concentrated under vacuum. Compound **HPQF 2** was isolated using a silica gel chromatographic column eluted with petroleum ether/Dichloromethane/ethyl acetate (v/v/v, 50:45:5), resulting a light yellow solid (R_f = 0.5, 292 mg, yield: 37%). ^{1}H NMR (500 MHz, $CDCl_3$): δ = 14.45 (s, 1H, N-H), 8.40 (d, J = 7.8 Hz, 1H, Ar-H), 8.19 (d, J = 8.1 Hz, 1H, Ar-H), 7.87 (d, J = 8.3 Hz, 1H, Ar-H), 7.82 (t, J = 7.2 Hz, 1H, Ar-H), 7.53 (t, J = 7.4 Hz, 1H, Ar-H), 7.38 (t, J = 7.5 Hz, 1H, Ar-H), 7.05 (d, J = 8.1 Hz, 1H, Ar-H), 6.96 (t, J = 7.4 Hz, 1H, Ar-H), 1.67 (q, J = 7.5 Hz, 3H, -SiCH$(CH_3)_2$), 1.20 (d, J = 7.5 Hz, 18H, -CH_3). ^{13}C NMR (125 MHz, $CDCl_3$): 166.36, 162.10, 161.38, 149.56, 134.28, 132.79, 129.35, 126.71, 126.15, 124.51, 119.25, 118.62, 117.80, 116.44, 18.12, 12.80. Anal. HPLC: 97.8% purity. Anal. Calcd for $C_{23}H_{30}N_2O_2Si$: C, 69.81; H, 7.56; N, 7.31. Found: C, 70.01; H, 7.66; N, 7.10. *ESI*-MS: *m/z* 395.4 $[M+H]^+$, 417.4 $[M+Na]^+$.

2-(2′-tert-butyldiphenylsilyloxy-phenyl)-4(3H)-quinazolinone (**HPQF 3**): To a solution of 2-(2′-hydroxy-phenyl)-4(3H)-quinazolinone **HPQ** (476 mg, 2.0 mmol) in anhydrous CH_2Cl_2 (40 mL), DMAP (4-dimethylamiopryidine, 30 mg) and triethylamine (1.5 mL) were added. The resulting mixture was cooled to 0 °C, and TBDPSCl (tert-butyldiphenylsilyl chloride, 822 mg, 3.0 mmol, in 10 ml CH_2Cl_2) was added in 3 portions over 30 min. The suspended mixture was slowly dissolved at room temperature with another 1 h. Then it was poured into the saturated $NaHCO_3$ (40 mL) solution, and the resulting mixture was extracted three times with CH_2Cl_2 (40 mL). The combined organic layer was dried over anhydrous Na_2SO_4, and concentrated under vacuum. Compound **HPQF 3** was isolated using a silica gel chromatographic column eluted with petroleum ether/Dichloromethane/ethyl acetate (v/v/v, 50:45:5), resulting a light yellow solid (R_f = 0.42, 171 mg, yield: 18%). ^{1}H NMR (500 MHz, $CDCl_3$): δ = 14.03 (s, 1H, N-H), 8.39 (d, J = 8.1 Hz, 1H, Ar-H), 7.87 (t, J = 8.7 Hz, 2H, Ar-H), 7.82 (d, J = 7.2 Hz, 4H, Ar-H), 7.60 (t, J = 6.5 Hz, 1H, Ar-H), 7.43 (t, J = 7.4 Hz, 2H, Ar-H), 7.38 (t, J = 7.4 Hz, 4H, Ar-H), 7.32 (d, J = 7.9 Hz, 1H, Ar-H), 7.32 (d, J = 7.9 Hz, 1H, Ar-H), 7.22 (d, J = 7.1 Hz, 1H, Ar-H), 6.92 (d, J = 8.2 Hz, 1H, Ar-H), 6.57 (t, J = 7.6 Hz, 1H, Ar-H), 1.28 (s, 9H, -Si $(CH_3)_3$). ^{13}C NMR (125 MHz, $CDCl_3$): 165.61, 161.72, 160.90, 149.90, 135.34, 134.38, 132.59, 132.06, 130.06, 129.88, 127.79, 126.84, 126.36, 124.30, 118.95, 118.23, 117.22, 116.34, 27.07, 19.74. Anal. HPLC: 99.4% purity. Anal. Calcd for $C_{30}H_{28}N_2O_2Si$: C, 75.51; H, 5.78; N, 5.91. Found: C, 75.60; H, 5.92; N, 5.88. *ESI*-MS: *m/z* 477.2 $[M+H]^+$, 499.1 $[M+Na]^+$.

Reaction probe **HPQF3** with NaF or TBAF (HPLC-MS positive ion mode): **HPQF3** (95.2 mg, 0.2 mmol) was dissolved in 50% CH_3CN/H_2O (100 mL) and followed by the addition of NaF (420 mg, 10.0 mmol) or TBAF (315 mg, 1.0 mmol). The reaction mixture was stirred at room temperature for 2 h and conversion was checked by analytical HPLC. (HPQ yield: > 80%) (4.6 mm × 150 mm 5 μm C18 column; 5 μL injection; 10% CH_3CN/H_2O, linear gradient, with constant 0.1% v/v TFA additive; 20 min run; 1 mL/min flow; ESI; positive ion mode; UV detection at 254 nm); *ESI*-MS: *m/z* 239.1 $[M+H]^+$, 261.1 $[M+Na]^+$.

3. Results and discussion

3.1. Rational design of the HPQ-based fluorescent probes

2-(2′-hydroxy-phenyl)-4(3H)-quinazolinone (HPQ) is distinguished

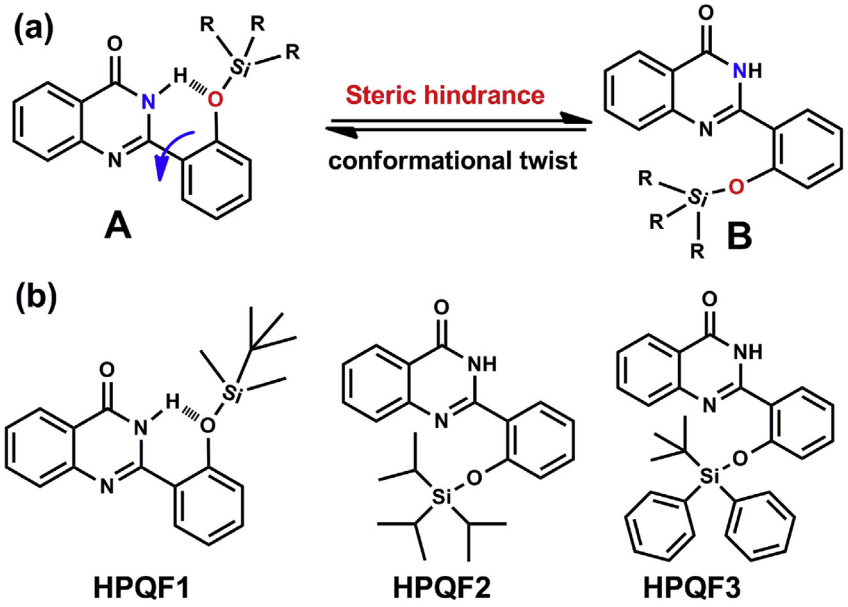

Scheme 1. Proposed Molecular conformations of HPQF1 ~ HPQF3 based on steric hindrance.

from common fluorescent dyes by its favorable photophysical properties, such as large Stokes shifts and excellent photostability [14]. Significantly, excited state intramolecular proton transfer is processed between its phenolic hydrogen and imine nitrogen, thereby assuring effective fluorescence quenching when phenolic hydrogen is substituted [15]. Such mechanism-based fluorophore have been employed in the design of water-soluble enzymes probes including alkaline phosphatase [14a], β-glucuronidase [14b], monoamine oxidases [14e], and acyl hydrolase [14d]. Herein, we designed three *turn-on* type probes for fluoride HPQF1 ~ HPQF3, which employed HPQ as the fluorophore and silyl ether groups as the detector. This design can also provide three silyl ethers with different steric hindrance, making it possible to study their influences on the probes' conformation and the sensing behavior with fluoride (Scheme 1b).

3.2. The possibility for conformational isomerism of the fluorescent probes

The ^{1}H NMR of HPQF1 ~ HPQF3 appeared two sets of amide hydrogen assignments (For HPQF1: 10.73 ppm; For HPQF2 and HPQF3: > 14.00 ppm), which motivated us to propose the different conformational isomerisms. HPQF1 may tend to form intramolecular hydrogen bond between the silyl-ether oxygen and the amide hydrogen (A-conformation) and thus was more stable than the extreme steric hindrance conformation. However, with greater steric hindrance, the silyl-ethers' substituents became slightly staggered as a result of the twist, which alleviated steric hindrance to form B-conformation in HPQF2 and HPQF3 (Scheme 1a). The corroborative evidences for two different conformations were also confirmed by fluorescence spectrums and DFT calculations. Compared with HPQF2 and HPQF3, the fluorescence intensity of HPQF1 was respectively 4.4-fold and 2.4-fold stronger than that of HPQF2 and HPQF3.

For three HPQ-based probes, the different conformation isomers depend primarily on the rotation between HPQ fluorophore (Plane A) and silyl ethers (Plane B) (Scheme 2). Therefore, there exists a rotational energy barrier that needs to be overcome to from one conformer to another. In order to find the energy minimum, we scan the conformations with dihedral angles of 0°–180° (every 15°) between Plane A and Plane B. As depicted in Fig. 1, the calculated tautomerization energy of A-conformation (the dihedral angle = 0°) is 12.44 kcaL/mol lower than B-conformation and hence provides the largest driving force for forming an intramolecular hydrogen bond. Compared with HPQF1, the tautomerization energy of B-conformation to A-conformation in HPQF2 and HPQF3 were estimated as 0.36 kcaL/mol and 1.01 kcaL/mol (Table 1), respectively. Thus, considering the steric hindrance and H-bond interaction, Those results may support the hypothesis that the two different conformational isomerisms exist in the three HPQ-based probes (see Scheme 3).

3.3. Detection of TBAF in CH_3CN and water

All three probes showed instant (< 30 s) *turn-on* response of TBAF in CH_3CN with a significant increase in fluorescence emission at 437 nm. The 1:1 stoichiometric of the desilylation mechanism was confirmed by titration experiments (Fig. S1, see Supporting Information). Interestingly, the emission maximum of probes with TBAF in HEPES buffer was red-shifted by 59 nm, probably due to the presence of ionic strength in the intramolecular hydrogen bond that increased the emission through energy transfer, as is commonly observed in ESIPT fluorophore [16]. Compared with Hong's probe [10a], the photophysical properties of HPQF1 ~ HPQF3 were stable in HEPES buffer for 24 h even the HPQ-based probes caused greater steric hindrance effect (Fig. S8 ~ S10, see Supporting Information). Upon interaction with TBAF, the titration reaction curves of HPQF2 and HPQF3 respectively showed a progressive fluorescence enhancement within 50 min (Φ_F = 0.34), and the fluorescence intensity were more than 80 times stronger than the blank (Fig. 2b). However, HPQF1 required a much longer time (> 160 min) to reach fluorescence intensity maximum (Fig. 2a), which may be explained by attributing the extra intramolecular H-bonding interaction. Additionally, the kinetic behavior of probes strongly demonstrated that the increasing steric hindrance around the silyl ether would cause the incremental fluorescence sensing behavior. As expected, the *pseudo*-first-order rate constants (Table 2) for HPQF1 ~ HPQF3 were determined as $k' = 4.45 \times 10^{-4}$ s^{-1}, 1.01×10^{-3} s^{-1}, and 1.38×10^{-3} s^{-1}, respectively. The detection limit (S/N = 3, Table 2) [17] of TBAF with HPQF3 was also determined to be 112 ppb, which was respectively 1.2-fold and 11.0-fold lower than that of HPQF2 and HPQF1 (Table 2). Therefore, we selected HPQF3 as a fluoride probe with excellent photophysical properties for the following investigation.

HPQF3 did not cause the observable fluorescent enhancement upon addition of many anions (100 equiv), such as Cl^-, Br^-, I^-, AcO^-, NO_3^- N_3^-, SCN^-, $H_2PO_4^-$ and HSO_4^- (Fig. 2c). Also, the interference

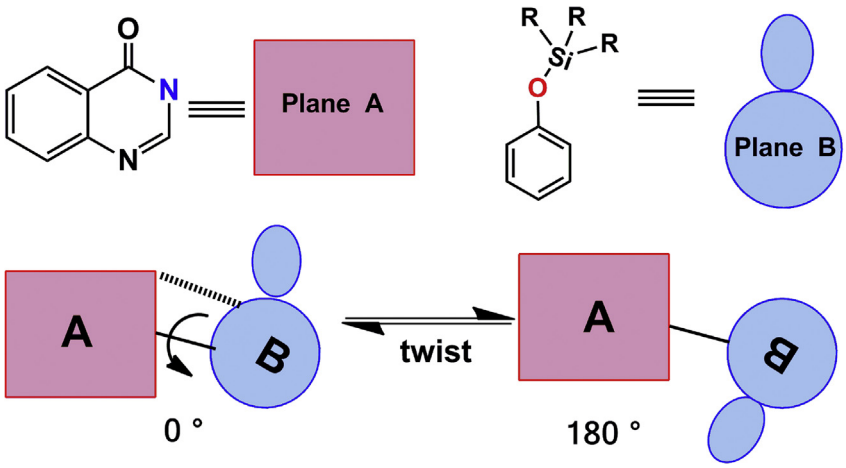

Scheme 2. HPQ fluorophore and silyl ethers were defined as Plane A and Plane B.

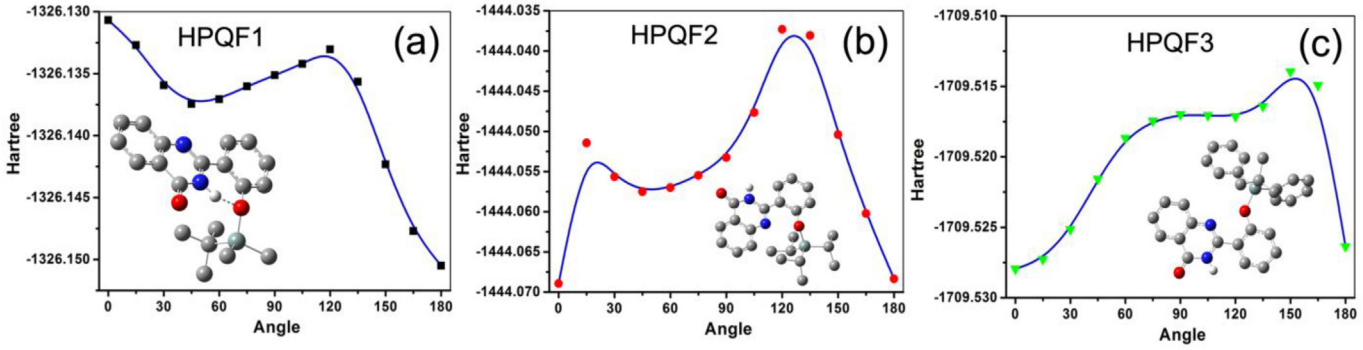

Fig. 1. The scanned Corresponding Energies (Optimization Geometries at the ground states) with dihedral angles of 0°–180° (every 15°) between Plane A and Plane B.

Table 1
Corresponding energy differences[a] (ΔE) between A-conformation and B-conformation for HPQF1 ~ HPQF3.

Probe	HPQF1	HPQF2	HPQF3
0° (hartree)	−1326.13068	−1444.06893	−1709.52796
180°(hartree)	−1326.15050	−1444.06835	−1709.52636
Δ*E* (kcal/mol)	−12.44	0.36	1.01

[a] Optimization Geometries at the ground states were calculated using B3LYP/6-31G(d,p) hybrid functional for all DFT computations.

experiments demonstrated consistent selectivity toward the above-mentioned analytes (Fig. 4b). The pH-dependent response experiments revealed that both HPQF3 and HPQF3/F^- elicited a negligible fluorescence intensity changes in the range of pH 6.43–8.07 (Fig. 4a), suggesting that HPQF3 was capable of working in physiological conditions.

The visual response of HPQF3 to various species demonstrated that HPQF3 can be conveniently employed for fluoride detection with two different fluorescent sensing channels in acetonitrile (blue) and water (green) by visual inspection (Fig. 3). Furthermore, the fluoride-promoted HPQF3 deprotection mechanism was confirmed by HPLC-MS and NMR (see Supporting Information). In the presence of TBAF or NaF, a complete peak at 361.1(*m/z*, HPQ) in MS spectrum manifested that HPQF3 irreversibly transformed to HPQ due to the fluoride desilylation.

3.4. Imaging fluoride in living cells

Since the HPQ-based probes exhibited excellent *turn-on* sensing behaviour of F^- in *aqueous* media, we next assessed whether HPQF3 was sensitive enough to monitor F^- in cellular environment. The mouse embryonic fibroblast (NIH3T3) cell line incubated with HPQF3 (5 μM, PBS medium) for 30 min (Fig. 5a) and 240 min (Fig. S10, see Supporting Information) at 37 °C showed only weak intracellular

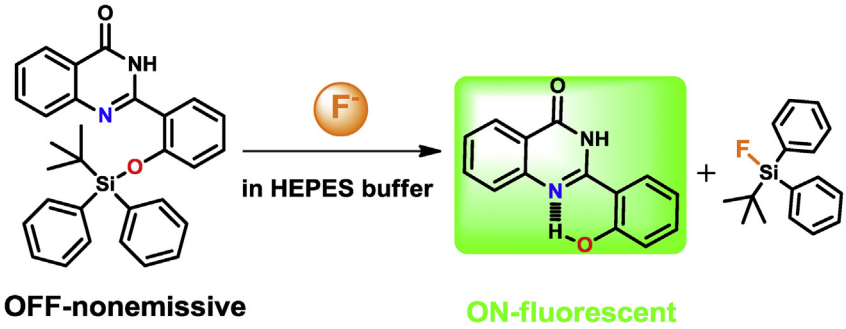

Scheme 3. *Turn-on* sensing mechanism of probe HPQF3 for the detection of fluoride.

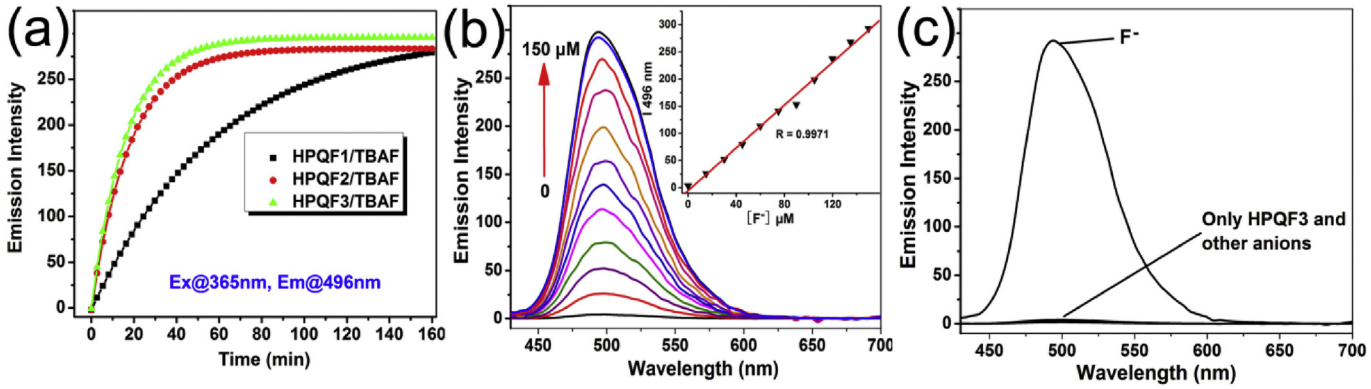

Fig. 2. (a) The time-dependent fluorescence changes acquired from reaction of HPQF1 ~ HPQF3 (2.0 μM) with TBAF (150 μM) in 20 mM HEPES buffer (pH 7.2, 1.5% DMSO) at 25 °C. (b) Fluorescence spectral changes of HPQF3 (2.0 μM) after the addition of TBAF (ranging from 0 to 150 μM). Inset: The fluorescence enhancement at 496 nm as a function of TBAF concentration. (c) Fluorescence responses of HPQF3 (2.0 μM) with various anions: Cl^-, Br^-, I^-, AcO^-, NO_3^- N_3^-, SCN^-, $H_2PO_4^-$ and HSO_4^-.

Table 2
The comparison of the sensing behavior and rate constants of HPQF1 ~ HPQF3.

Probe	HPQF1	HPQF2	HPQF3
N-H (ppm)[a]	10.73	14.45	14.03
F_{Max}/F_{ap}(TBAF)[b]	26.4-fold	81.2-fold	89.3-fold
F_{Max}/F_{ap}(NaF)[b]	stable	~5.1-fold	~6.0-fold
K′(s^{-1})[c]	4.45×10^{-4}	1.01×10^{-3}	1.38×10^{-3}
DL_{Water}[d]	1.23 ppm	129 ppb	112 ppb

[a] ^{1}H NMR spectra of N-H assignments were acquired in $CDCl_3$ at 298 K.
[b] The relative emission intensity of HPQF1 ~ HPQF3 with TBAF(NaF, 3 h) compared to the blank probe.
[c] The *pseudo*-first-order rate constant of HPQF1 ~ HPQF3 with TBAF.
[d] The detection limit of TBAF with HPQF1 ~ HPQF3 were determined on the basis of S/N = 3 method.

fluorescence, indicating HPQF3 was photophysical stable under biological conditions. In contrast, the probe-loaded cells were treated by the followed 100 μM TBAF incubation for 120 min and a significant enhancement was observed in intracellular fluorescence (Fig. 5c). The TBAF-loaded cells only triggered ~20% of the total fluorescence intensity within 30 min due to the slow rate of cleavage reaction in living cells (Fig. 5b). These results indicated that HPQF3 was a good membrane-permeable probe and can reliably detect intracellular fluoride level changes in living cells. Additionally, the MTT assay showed the cell viability only declined ~7.4% (Fig. S12, see Supporting Information) upon 5 μM HPQF3 treatment (8 h), thus clearly demonstrated that HPQF3 has low toxicity to the cultured cell lines under the staining experiment.

3.5. Imaging fluoride in different zebrafish organelles

Zebrafish has been proved as a prominent model organism for vertebrate development and gene function [18]. Recently, Bartlett demonstrated that fluoride exposure for zebrafish could lead to perturbations in growth factor signaling and apoptosis [19]. Therefore, zebrafish was adopted as the imaging model to investigate the accumulating behavior of fluoride in different organelles. Three-month-old zebrafish with identifiable organs was exposed to 200 μM TBAF in E3 embryo media for 8 h accumulating fluoride in organs. All of the fish survived, thus indicating that 8 h LC_{50} value of zebrafish is much higher than 200 μM. The prolonged time exposure to fluoride may make organ

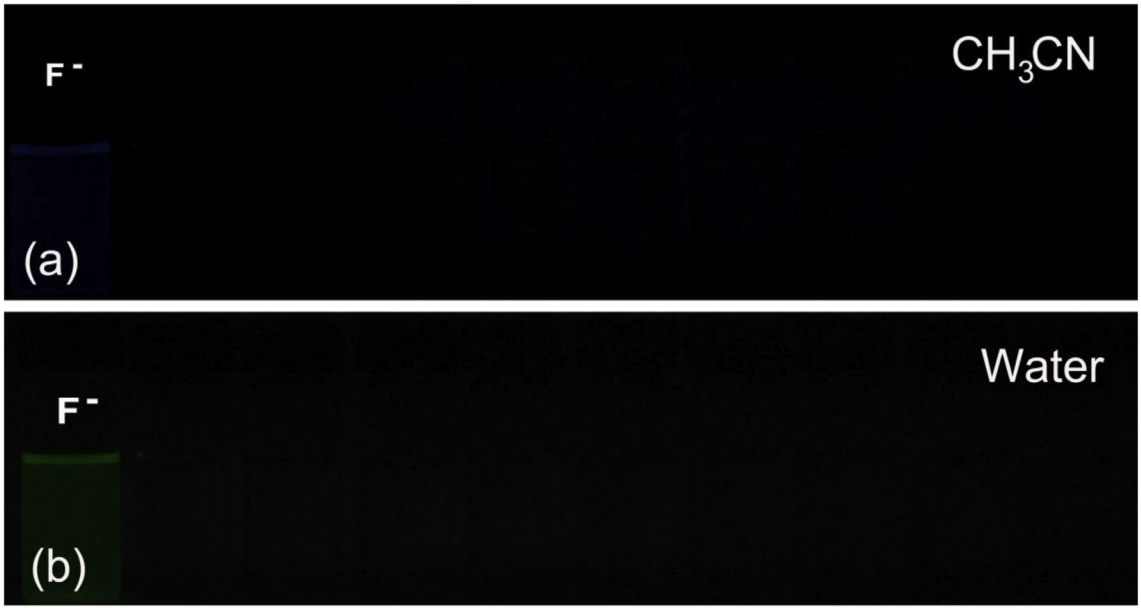

Fig. 3. Fluorescent images of HPQF3 (5 μM) in CH_3CN (a) and in HEPES buffer (b) upon addition of various anions: F^-, Cl^-, Br^-, I^-, AcO^-, NO_3^- N_3^-, SCN^-, $H_2PO_4^-$ and HSO_4^-.

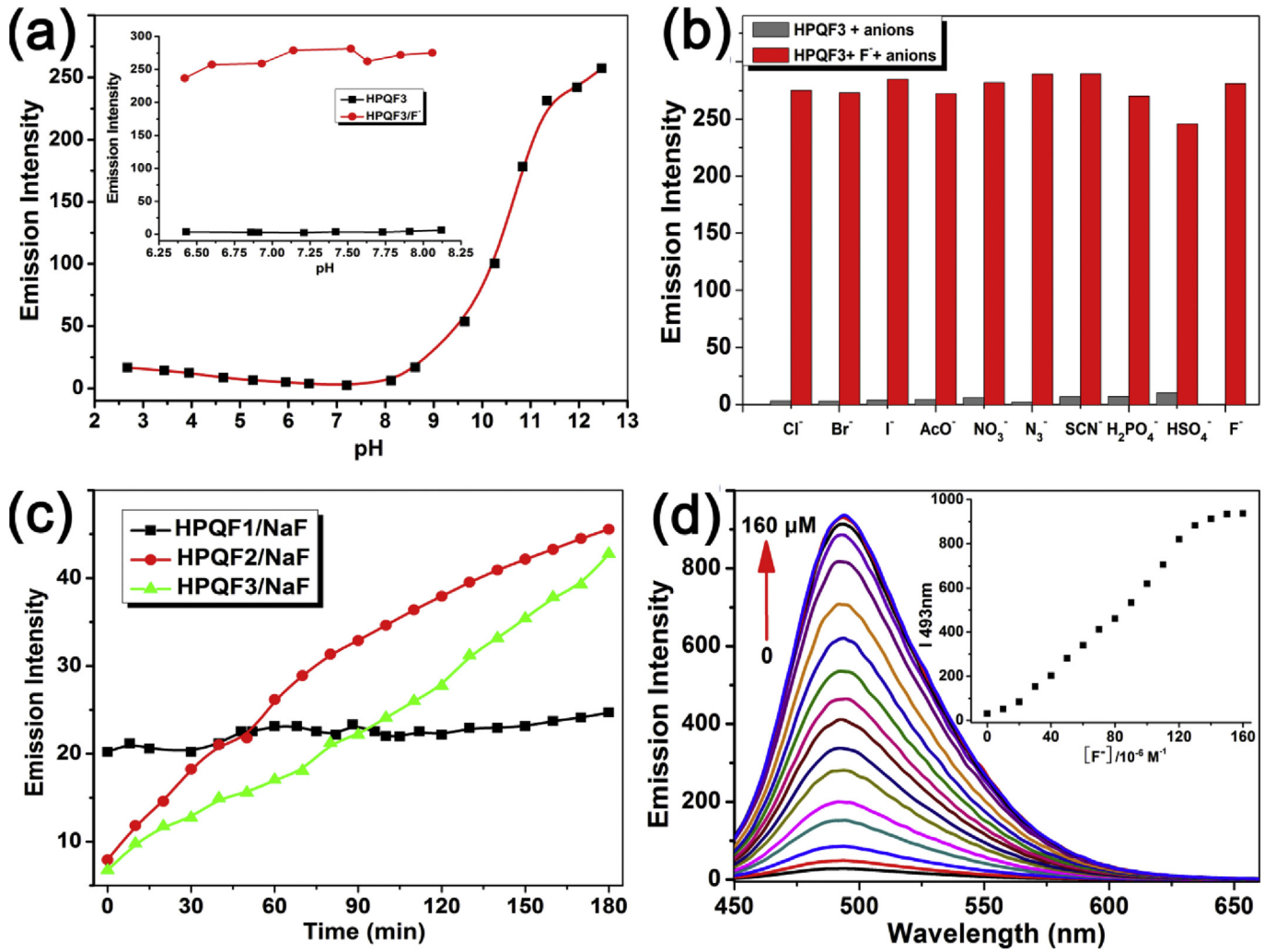

Fig. 4. (a) Fluorescence response of HPQF3 (2.0 μM) to various anions: Cl^-, Br^-, I^-, AcO^-, NO_3^- N_3^-, SCN^-, $H_2PO_4^-$ and HSO_4^-. Spectra were acquired in HEPES buffer (pH 7.2, 1.5% DMSO) at 25 °C. The gray bars represent the addition of the competing anion to a 2 μM solution of HPQF3. The red bars represent the change of the emission that occurs upon the subsequent addition of 150 μM F^- to the above solution. (b) Fluorescence responses of probe HPQF3 and HPQF3/F^- at different pH. (c) The time-dependent fluorescence changes acquired from reaction of HPQF1 ~ HPQF3 (4.0 μM) with NaF (2.0 mM) in HEPES buffer (pH 7.2, 2.5% DMSO) at 25 °C. (d) Fluorescence spectral changes of HPQF3 (5.0 μM) after the addition of NaF (ranging from 0 to 160 μM) in aqueous DMF solution (HEPES, 20 mM, pH = 7.0, 7: 3, v/v). Inset: The fluorescence enhancement at 493 nm as a function of NaF concentration. (For interpretation of the references to colour in this figure legend, the reader is referred to the Web version of this article.)

deformation or even lead to death. Then, the treated zebrafish was incubated with 2 μM HPQF3 for 60 min, which was further dissected to isolate tissues and organs. The fluorescent signals can be detected in the eye, heart, brain, eggs, and liver, and intensively monitored in intestine and gall bladder by HPQF3 (Fig. 6). The average emission intensities of isolated organs were analyzed by IPP software and the intensities were suggested in the order: gall bladder > intestine > eggs > heart > eye > brain > liver (Fig. S13, see Supporting Information). These results demonstrated that HPQF3 was capable of monitoring the sites of fluoride ion accumulation in zebrafish.

3.6. Detection of NaF in water and toothpaste samples

Since the most of the common fluorides are inorganic in nature, we also investigated the same titration experiment with NaF in HEPES buffer. Unfortunately, HPQF1 did not show any fluorescent response upon addition of 1 mM F^-, and also HPQF2 and HPQF3 showed only 6.5-fold and 2.4-fold enhancement of fluorescence intensity respectively after 3 h treatment of 2 mM F^- (Fig. 4c), which was comparable to that of the silyl ether-coumarin based probes [10]. However, this weak fluorescence signal is insufficient to detect inorganic fluoride in water samples. We examined the concentration of HPQF3 and the reaction media to optimize the detection system. The results showed that the response signals increased with the use of increasing volume of DMF as a co-solvent. Upon the addition of NaF to 5 μM HPQF3 in *aqueous* DMF solution (HEPES, 20 mM, pH = 7.0, 7: 3, v/v), a significant increase (32.6-fold) in the fluorescence intensity at 493 nm was observed (Fig. 4d) when excited at 365 nm. A nearly linear relationship between the fluorescence intensity and concentration of NaF was observed for a wide concentration range (0–160 μM). The LOD at an S/N ratio of HPQF3 for NaF was 327.9 ppb, which is lower than the maximum level of fluoride in drinking water permitted by the United States Environmental Protection Agency (EPA) [10b].

The practical application of HPQF3 was employed to determine fluoride concentrations in sample from XuanWu lake and the commercial toothpaste (Crest). The water samples were filtered by cellulose acetate membranes prior to use, and then spiked with NaF at different concentrations of 0.95 mg/L, 1.90 mg/L, and 2.85 mg/L. As shown in Table 3, the results obtained with the proposed fluorescent method were in good agreement with those obtained by the fluoride-ion

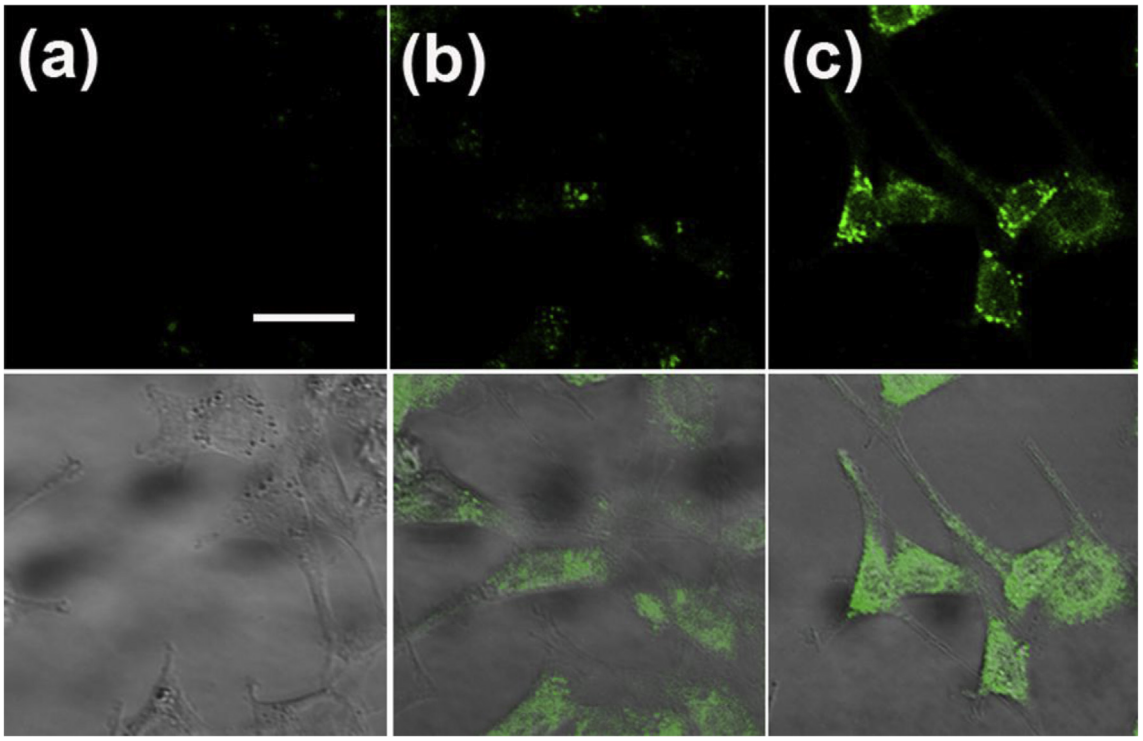

Fig. 5. Confocal microscopy images of NIH3T3 cells (a) incubated with 5 μM HPQF3 for 1 h at 37 °C in PBS buffer (1.5% DMSO as a co-solvent); incubated with 100 μM TBAF prior to HPQF3 staining for 30 min (b) and 120 min (c) at 37 °C. Bottom: overlay bright field images in (a), (b) and (c). The scale bar represents 30 μm.

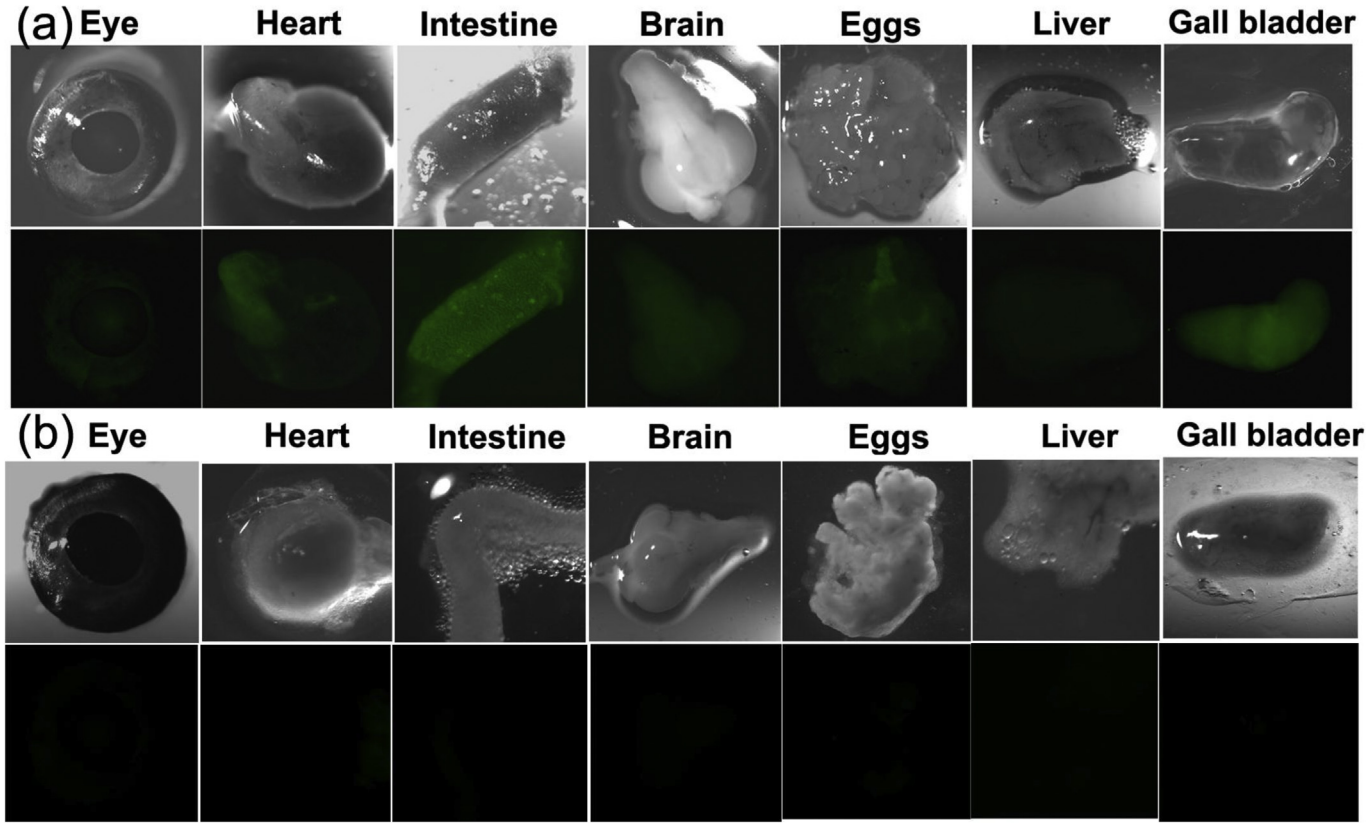

Fig. 6. Images of adult zebrafish organs treated with 2 μM HPQF3 in the (a) presence (1.5 h) and (b) absence of external TBAF in E3 embryo media (1.5% DMSO as a co-solvent) for 8 h at 28.5 °C. The images were collected on a fluorescent dissecting microscope (Leica) equipped with a DP70 digital imaging system (Olympus) with a GFP filter set. The average emission intensities of isolated organs were analyzed by using IPP software.

Table 3
Determination of the Concentrations of NaF in water and toothpaste samples by florescent and fluoride-ISE method.

Samples	florescent method	ISE method
Water 1	0.932 ± 0.036 mg/L	0.96 ± 0.014 mg/L
Water 2	1.844 ± 0.113 mg/L	1.889 ± 0.060 mg/L
Water 3	2.747 ± 0.149 mg/L	2.827 ± 0.105 mg/L
Toothpaste 1	0.874 ± 0.065 mg/g	0.982 ± 0.031 mg/g
Toothpaste 2	0.913 ± 0.047 mg/g	1.124 ± 0.029 mg/g

Average value of three determinations (± S.D.).

selective electrode (ISE) method (relative error less than 4%). Sodium fluoride is the most common source for the additional fluoride in toothpaste, which has the beneficial effects on the formation of dental enamel and bones. The fluoride concentrations in commercial toothpastes determined by this approach were also in accordance with those obtained by fluoride-ISE method, which further verified that HPQF3 is applicable for practical fluoride detection.

4. Conclusion

In summary, we have developed three *turn-on* fluorescent fluoride probes HPQF1 ~ HPQF3 based on the great affinity between fluoride and silicon. Among these three probes, the different steric hindrance around the silyl ethers strongly influenced the probes' conformation and the sensing behavior with fluoride. The three HPQ-based probes can quantitatively detect fluoride anion concentration in acetonitrile as well as in water. The fluorescent response time was only few seconds in acetonitrile, and we were able to easily observe two different fluorescent sensing channels in acetonitrile and water by naked eyes. HPQF3 exhibited an 89.3-fold fluorescence enhancement, high selectivity, and pH-independent sensing ability toward fluoride anions in physiological conditions. This work also provided a useful method to monitor fluoride in both living cells and specific organelles in zebrafish.

Acknowledgment

This work is supported by the Natural Science Foundation of Jiangsu Province (BK20170996), the Natural Science Key Fund for Colleges and Universities of Jiangsu Province (15KJB530006).

Appendix A. Supplementary data

Supplementary data related to this article can be found at http://dx.doi.org/10.1016/j.dyepig.2018.05.053.

References

[1] (a) Beer PD, Gale PA. Angew Chem, Int Ed 2001;40:486–516;
(b) Sessler JL, Gale PA, Cho WS. Anion receptor Chemistry. Cambridge, UK: Royal Society of Chemistry; 2006.
[2] Kirk KL. In biochemistry of the elemental halogens and inorganic halides. New York: Plenum Press; 1991. p. 19–68.
[3] (a) Cittanova ML, Lelongt B, Verpont MC, Geniteau-Legendre M, Wahbe F, Prie D, Coriat P, Ronco PM. Anesthesiology 1996;84:428–35;
(b) Singh PP, Barjatiya MK, Dhing S, Bhatnagar R, Kothari S, Dhar V. Urol Res 2001;29:238–44;
(c) Carton RJ. Fluoride 2006;39:163–72.
[4] (a) Yang JY, Baker CA, Ward JR. Chem Rev 1992;92:1729–43;
(b) Housecroft CE, Sharpe AG. Inorganic Chemistry. third ed. Harlow: Pearson Education Ltd; 2008. p. 872–3.
[5] (a) Mizuno T, Wei WH, Eller LR, Sessler JL. J Am Chem Soc 2002;124:1134–5;
(b) Cho EJ, Moon JW, Ko SW, Lee JY, Kim SK, Yoon J, Nam KC. J Am Chem Soc 2003;125:12376–7;
(c) Boiocchi M, Boca LD, Esteban-Gomez D, Fabbrizzi L, Licchelli M, Monzani E. J Am Chem Soc 2004;126:16507–15;
(d) Vazquez M, Fabbrizzi L, Taglietti A, Pedrido RM, Gonzalez-Noya AM, Bermejo MR. Angew Chem, Int Ed 2004;43:1962–5;
(e) Chang KJ, Moon D, Lah MS, Jeong KS. Angew Chem, Int Ed 2005;44:7926–9;
(f) Gu B, Zhang Q. Adv Sci 2018;5:1700609;
(g) Gu PY, Wang Z, Zhang Q. J Mater Chem B 2016;4:7060–74.
[6] (a) Liu Z, Shi M, Li F, Fang Q, Chen Z, Yi T, Huang C. Org Lett 2005;7:5481–4;
(b) Swamy KMK, Lee YJ, Lee HN, Chun J, Kim Y, Kim SJ, Yoon J. J Org Chem 2006;71:8626–8;
(c) Liu XY, Bai DR, Wang S. Angew Chem, Int Ed 2006;45:5475–8;
(d) Chiu C, Gabbaï FP. J Am Chem Soc 2006;128:14248–9;
(e) Hudnall TW, Gabbaï FP. Chem Commun 2008;44:4596–7;
(f) Neelakandan PP, Ramaiah D. Angew Chem Int Ed 2008;47:8407–11;
(g) Kim Y, Gabbaï FP. J Am Chem Soc 2009;131:3363–9.
[7] (a) Kim SY, Hong J. J Org Chem 2007;75:3109–12;
(b) Hum R, Feng J, Hu D, Wang S, Li S, Yang G. Angew Chem, Int Ed 2010;49:4915–8;
(c) Zhu B, Yuan F, Li R, Li Y, Wei Q, Ma Z, Du B, Zhang X. Chem Commun 2011;47:7098–100;
(d) Zhang JF, Lim CS, Bhuniya S, Cho BR, Kim JS. Org Lett 2011;13:1190–3;
(e) Zhu B, Yuan F, Li R, Li Y, Wei Q, Ma Z, Du B, Zhang X. Chem Commun 2011;47:7098–100;
(f) Kim D, Singha S, Wang T, Seo E, Lee JH, Lee SJ, Kim KH, Ahn KH. Chem Commun 2012;48:10243–5.
[8] Dalapati S, Alam MA, Saha R, Jana S, Guchhait N. Cryst Eng Comm 2012;14:1527–30.
[9] Kim T, Swager TM. Angew Chem, Int Ed 2003;42:4803–6.
[10] (a) Kim SY, Park J, Koh M, Park SB, Hong J. Chem Commun 2009;45:4735–7;
(b) Sokkalingam P, Lee C. J Org Chem 2011;76:3820–8.
[11] Yang XF, Qi H, Wang L, Su Z, Wang G. Talanta 2009;80:92–7.
[12] Yang YK, Ko SK, Shin I, Tae J. Nat Protoc 2007;2:1740–5.
[13] Yang XF, Ye SJ, Bai Q, Wang XQ. J Fluoresc 2007;17:81–7.
[14] (a) Huang ZJ, Terpetschnig E, You WM, Haugland RP. Anal Biochem 1992;207:32–9;
(b) Zhou MJ, Upson RH, Diwu Z, Haugland RP. J Biochem Biophys Methods 1996;33:197–205;
(c) Haugland RP. J Biochem Biophys Methods 1996;33:197–205;
(d) Diwu Z, Lu YX, Upson RH, Zhou MJ, Klaubert DH, Haugland RP. Tetrahedron 1997;53:7159–64;
(e) Zhang XB, Waibel M, Hasserodt J. Chem Eur J 2010;16:792–5;
(f) Aw J, Shao Q, Yang Y, Jiang T, Ang C, Xing B. Chem Asian J 2010;5:1317–21.
[15] (a) Heller A, Williams DL. J Phys Chem 1970;74:4473–80;
(b) Tolbert LM, Solntsev KM. Acc Chem Res 2002;35:19–27.
[16] Catalan J, Fabero F, Guijarro MS, Claramunt RM, Maria MDS, Focesfoces MD, Cano FH, Elguero J, Sastre R. J Am Chem Soc 1990;112:747–59.
[17] Lohani CR, Kim JM, Chung SY, Yoon J, Lee KH. Analyst 2010;135:2079–84.
[18] (a) Ko SK, Chen X, Yoon J, Shin I. Chem Soc Rev 2011;40:2120–30;
(b) Zhou Y, Li JY, Chu KH, Liu K, Yao C, Li JY. Chem Commun 2012;48:4677–9.
[19] Bartlett JD, Dwyer SE, Beniash E, Skobe Z, Payne-Ferreira TL. J Dent Res 2005;84:832–6.